Transactions, SMiRT-24
BEXCO, Busan, Korea - August 20-25, 2017
Division III

FIRST STRUCTURE MECHANICAL SIMULATIONS OF THE VERCORS PRE-STRESSED CONCRETE CONTAINMENT MOCK-UP

Ludwig Bahr[1], Jürgen Sievers[2]

[1] Expert Structure Mechanics, GRS (Gesellschaft für Anlagen- und Reaktorsicherheit), Germany
[2] Chief Expert Structure Mechanics, GRS (Gesellschaft für Anlagen- und Reaktorsicherheit), Germany

ABSTRACT

A mock-up of a French type pre-stressed concrete containment vessel without liner at 1:3-scale was built at Renardières near Paris, France, by Électricité de France (EDF) to investigate leak tightness of the structure. EDF invited international participants to take part in a simulation benchmark dedicated to investigate early-age concrete behavior, structure mechanical behavior and leak tightness in response to internal pressurization.
Structure mechanical analyses simulating the pressurization experiments of the reactor building using the finite element program LS-DYNA are presented. The simulations include the tensioning, anchoring and grouting of the tendons and the subsequent pressurization of the containment up to design pressure. All tendons are modelled individually. The concrete structure including the reinforcement is modelled with layered shell elements. Displacements measurements on the outside of the containment building as well as concrete strain measurements, which were recorded throughout the experiment, are compared to simulation results. Evaluating the structure mechanical simulation, crack opening displacements (COD) and crack opening areas (COA) are derived from the damaged concrete regions within the structure. They are used in calculating the leak rate due to internal overpressure with multiple analytical methods. Results are compared to localized leak rates, which were measured during the pressurization test.
The work of GRS was carried out in the framework of the German reactor safety research program funded by the German Federal Ministry of Economic Affairs and Energy (BMWi).

INTRODUCTION

Considering nuclear power plants, the last physical barrier in a series of barriers to retain the uncontrolled release of radioactivity in case of a severe accident is the containment vessel. Hence, design and building codes demand leak-tightness of the structure; in addition leak-tightness is checked during the operational life of nuclear power plants in the framework of in-service inspections. Profound investigations of the integrity of containment vessels have been performed to this day. Hessheimer and Dameron (2006) give an overview of containment integrity research performed at Sandia National Laboratories (SNL) and other institutions worldwide.
The experimental program executed on Sandia National Laboratories' 1:4-scale pre-stressed concrete containment vessels model was accompanied by extensive pre-test and post-test round robin simulation benchmarks including the International Standard Problem No. 48 (ISP 48) organized by the Committee on the Safety of Nuclear Installations (CSNI, 2004), an organizational unit of the OECD Nuclear Energy Agency. Construction and testing took place from 1997 until 2002; an extensive report on the experimental program was composed by Hessheimer et al. (2003). GRS contributed containment integrity calculations to ISP 48; further investigations were presented by Grebner and Sievers (2005). In 2010, an international round robin simulation benchmark was initiated by the U.S. Nuclear Regulatory Commission (NRC) and the Atomic Energy Regulatory Board (AERB) of India under the name Standard Problem Exercise #3 (2010). It was based on the experimental results of Sandia National Laboratories'

1:4-scale model. Investigations and simulation results performed at GRS were presented by Bahr and Sievers (2013).

VeRCoRs containment mock-up

In 2014 EDF started to build a containment vessel model at 1:3-scale at "EDF Lab Les Renardières" near Paris, France, to further investigate the integrity of containment structures and challenges regarding lifetime extension. The construction consists of a pre-stressed and reinforced concrete containment vessel within a secondary reinforced concrete building both on top of a thick concrete block foundation. Figure 1 shows a sectional view of the building. The inner containment exhibits a cylindrical wall founded on a cylindrical base slab. At the intersection a 0.67 m tall wall segment is thickened, the so-called gusset. Between torispherical dome and cylindrical wall lies the ring girder (toric belt), where dome tendons, gamma-shaped tendons and vertical tendons are anchored.

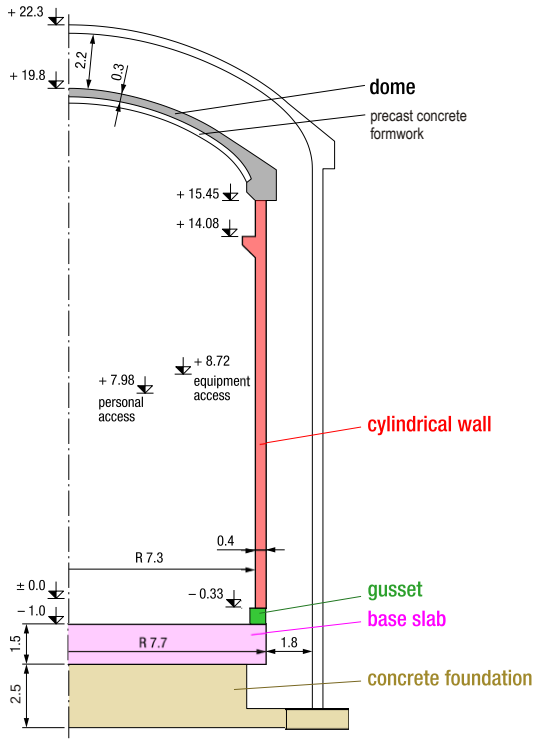

Figure 1: Main parts of the VeRCoRs containment mock-up.

Only two structurally significant penetrations have been included in the inner containment: the equipment hatch with a diameter of 2.71 m and the personal airlock with a diameter of 1.21 m. Other minor penetrations are not reproduced in the model, but two smaller ones with a diameter of 0.50 m and 0.36 m are added in order to insert pressurization pipes. Two vertical prestressing buttresses of the inner containment, where the horizontal tendons are anchored, are included as well.
Concrete of class 34/37 MPa is used for the construction. Material parameters are determined on-site as well as from samples in the laboratory. The prestressing tendons layout is exactly scaled, including any deviations around penetrations. Every tendon has been cement grouted as in the full-scale structure. The prestressing tendons are composed of class 1860 MPa T15 strands with a nominal cross-sectional area of 139 mm². Each tendon has been tensioned at 1488 MPa before anchorage slip, as in the full-scale structure.

Steel class 500 MPa has been used in the reinforcement. Rebar spacing and rebar diameters are scaled to keep the same reinforcement ratios compared to the full-size structure. Within the cylindrical wall away from penetrations, there are alternately 6 mm and 8 mm diameter rebars with a spacing of 6.7 cm in horizontal direction at both inner and outer face, as well as 8 mm and 10 mm diameter rebars with an angular spacing of 0.75° in vertical direction. Around penetrations and near the anchoring buttresses the reinforcement density is significantly increased. In the dome region, there are alternately 8 mm and 10 mm diameter rebars with spacing of 9.8 cm in meridional and tangential direction at both the inner and outer faces. Stirrups have generally a diameter of 5 mm.

SIMULATION MODEL

Structure mechanical simulations were performed using the finite element program package LS-DYNA (2016). The simulation model was setup to reproduce the first pressurization test of the containment vessel model. Since the pressure was increased over the duration of 12 hours during the test procedure, dynamic effects are neglected. Although an explicit time-stepping is employed, the simulation period is chosen sufficiently long and global damping is applied to the model to suppress the dynamics. The simulation period is divided in 4 phases. In the first phase, the tendons are tensioned. During anchoring in the second phase, the tendons slip slightly through until the ends are fully jammed. Tendon stress is slightly reduced towards the tendon ends. During the third phase the internal pressure acting upon the inner surface is increased up to design pressure of 5.2bar (absolute). In the fourth phase the internal pressure is held constant similar to the test procedure.
The concrete structure with the embedded reinforcement is modelled by multilayer thick shell elements utilizing MAT_172 Eurocode 2 concrete model. Vertical and horizontal reinforcement is modelled through respective layers of the shell elements. Figure 2(a) shows an isometric view of the finite element model. Until now the foundation and the inner part of the base slab is omitted in the finite element model and the degrees of freedom of the lowermost shell elements are locked.

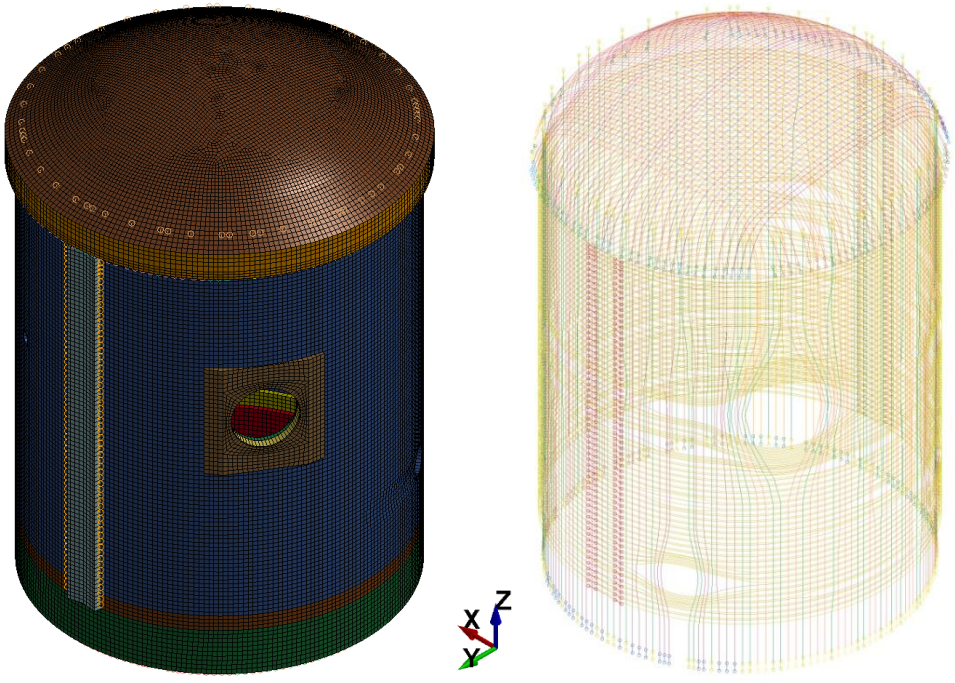

(a) (b)

Figure 2: Finite element model of the VeRCoRs inner containment vessel (a). Isometric view of the tendons and pre-stressing elements only (b).

The MAT_172 material model can represent plain concrete only, reinforcing steel only, or a smeared combination of concrete and reinforcement. The model includes concrete cracking in tension and crushing in compression as well as reinforcement yield, hardening and failure. The concrete is assumed to crack in tension when the maximum in-plane principal stress reaches the defined tensile strength. Figure 3 shows the stress-strain relationship of the material model. A non-rotating smeared crack approach is implemented. Cracks can open and close repeatedly under hysteretic loading. When a crack is closed it can carry compression according to the normal compressive stress-strain relationships. The direction of the crack relative to the respective element coordinate system is stored when the crack first forms. Details of the material model can be found in the LS-DYNA Keyword User's Manual (2016).

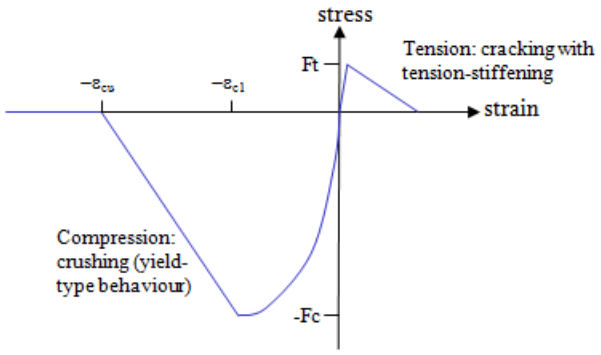

Figure 3: Stress-strain behaviour of the MAT_172 Eurocode 2 concrete model.

All 295 tendons of the inner containment structure, i.e. 18 dome tendons, 57 vertical tendons, 122 horizontal tendons and 98 gamma-shaped tendons, are modelled individually by beam elements. Figure 2(b) gives an isometric view of the elements representing the tendons. In the generation of the finite element model, the tendon elements are meshed on basis of a CAD file provided by EDF. The tendon elements are copied on the spot to form ducts in order to allow tangential sliding of tendon nodes along the guiding duct during the tensioning and anchoring process. A guided cable contact with friction is employed between tendon elements und duct nodes. The duct nodes themselves are tied to the surrounding concrete elements. Analogous to the grouting of the tendons, the tendon nodes are eventually tied to the concrete elements after the anchoring is complete. The tensioning and anchoring of the tendons is facilitated by axial force beam elements attached to the ends of the tendons. The model consists of 140000 beam elements and 45000 thick shell elements, which themselves have 8 layers to incorporate the reinforcement.

RESULTS

Simulation results are compared to experimental results published so far by EDF in the framework of the VeRCoRs simulation benchmark. Until today, radial displacement measurements on the outside of the inner containment as well as strain measurements at various locations within the concrete structure are made available to the participants of the simulation benchmark.
Four pendulums are installed around the outer surface of the inner containment at an angle of 48.2, 146.5, 274.5 and 368 gradians (1 gradian is 1/400 of a turn). Note, that the two anchoring buttresses on opposite sides are located at 95.5 gradians and 295.5 gradians. The centre axis of the equipment hatch is at 235.5 gradians. Radial displacement measurements are recorded at three levels, namely +4 m, +9 m and +14.8 m, which makes a total of 12 measurement locations. Figure 4 depicts the results. The simulation reproduces the pressurization process very well. The biggest deviations between simulation and measurement occur at the level of the equipment hatch between the hatch and the nearest anchoring

buttress located at 295.5 gradians mainly due to differences between the complex reinforcement layout in the mock-up and the modelling in the analysis model.

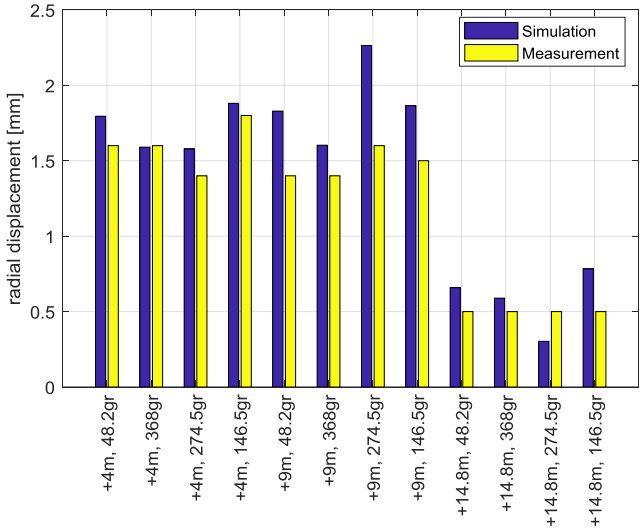

Figure 4: Comparison of simulated and measured radial displacements during the first pressurization test.

Several strain gauges were embedded in the concrete structure during the construction process. At each sensor location there are two strain gauges at an angle of 90 degrees (vertical and tangential strain) together with a thermometer to allow for a correction due to a different thermal dilation of concrete and sensor wire. Strain gauge readings were recorded from the start of the construction till this day at least every 12 hours. During periods of interest, e.g. the tensioning of the tendons and the pressurization tests, the recording interval was significantly shortened to 0.5 - 1 hour. In addition to the sensor labelling with a letter and a number, the orientation and the location of the sensor near the inner surface of the wall (Intrados) or the outer surface of the wall (Extrados) is specified. Figure 5 shows the strain gauge recording of the sensors G1 and G2, which are located at a level of -0.25 m and an angle of 172 gradians.

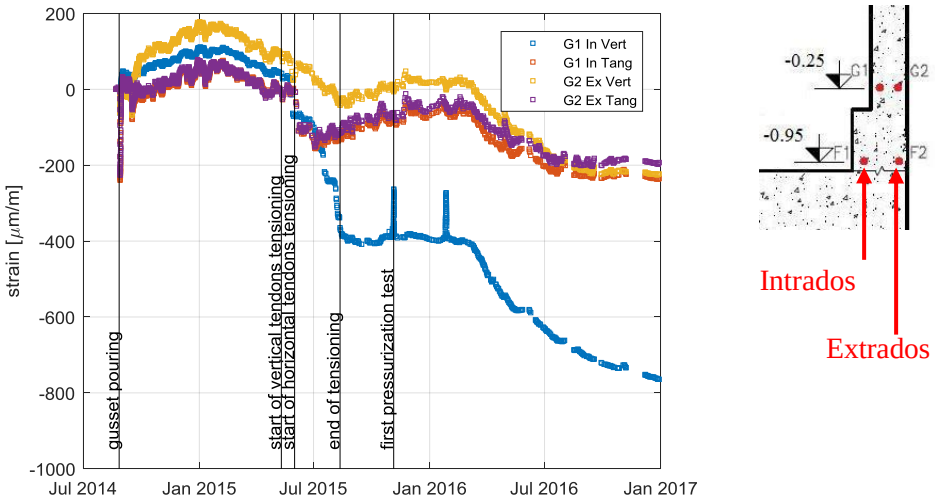

Figure 5: Concrete strain recording in vertical and tangential direction at sensors G1 and G2 (G1 Intrados Vertical, G1 Intrados Tangential, G2 Extrados Vertical and G2 Extrados Tangential).

The recording period dates from 21 August 2014 to 29 December 2016. Tensioning of the tendons began on 11 March 2015 and ended in 12 August 2015. Only the vertical strain at sensor G1 near the inner surface (Intrados) shows a strong decrease due to tensioning, strains near the outer surface (G2 Extrados) respond considerably less. The first pressurization test took place from 4 November to 5 November 2015. It can be identified as the first significant peak in the G1 Intrados Vertical gauge reading. On 4 November at 12:00 the internal pressure was linearly increased up to 5.2 bar (absolute) until midnight. From 5 November, 0:00 until 12:00 the internal pressure was held constant. Then the pressure was linearly decreased back to normal conditions. Inspecting the signals over the whole recording period, one can observe a significant signal drift, which is different for each sensor. It can partly be attributed to a temperature effects due to ambient climate conditions. Possible causes for the different behaviour of each sensor could be leakage currents, mechanical damage and corrosion.
In the following graphs selected simulated strain responses are compared to measured strain gauge readings. The measured gauge signals are displayed as they were recorded, that means they exhibit a significant offset compared to the simulated signals due to signal drift. Figure 6 depicts the vertical strain of the sensors F1, F2, G1 and G2. All of the sensors are located at an angle of 172 gradians, the sensors F1 and F2 are at a level of -0.95 m in the gusset region, the sensors G1 and G2 are at a level of -0.25 m slightly above the gusset region. Subtracting the offset from the measured strains, one observes, that strain values on the inside (Intrados) are simulated with greater accuracy than the strains near the outer surface (Extrados), i.e. the bending effect at the junction from base slab to cylinder wall is overestimated in the simulation model. Only the outer part of the base slab is included in the model. Furthermore, the controlled heat treatment of the gusset after the pouring of the concrete with the aim to generate cracks is not yet included in the simulation. Hence, the simulated strain values may deviate from the measured strains.

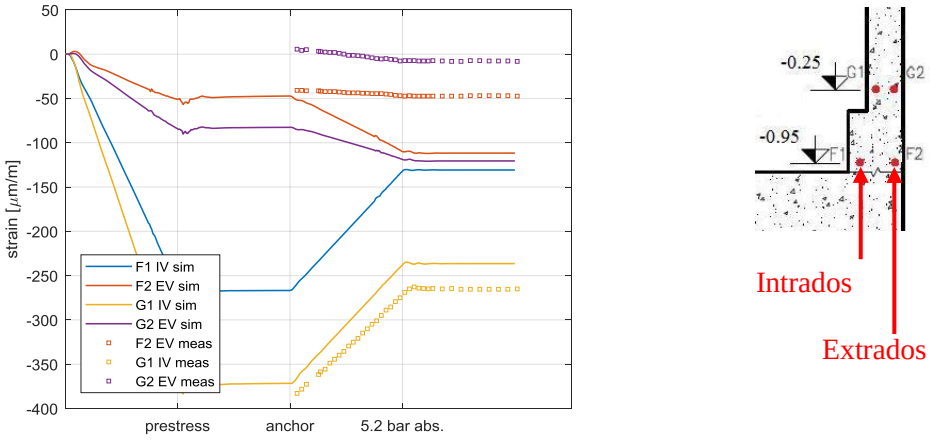

Figure 6: Comparison of simulated and measured vertical strain at sensors F1, F2, G1 and G2 (F1 Intrados Vertical, F2 Extrados Vertical, G1 Intrados Vertical and G2 Extrados Vertical).

Figure 7 shows the vertical strain and Figure 8 the tangential strain of the sensors H1, H2, H5 and H6, which are located at a level of +8 m at mid-height of the cylindrical containment wall. H1 and H2 are at an angle of 172 gradians, H5 and H6 on the opposite side of the cylinder wall at 368 gradians. Figure 9 shows the strain responses of the sensors I1 and I2 in x- and y-direction as well as the simulated strain values. They are located at a level of +19.8 m and +19.6 m at the zenith of the dome. The signal recordings of the sensors I1 and I2 show deviations from the linear pressure increase followed by the pressure plateau, which may indicate a poor sensor signal quality. Subtracting the sensor offset, the simulated strain values reproduce the vertical as well as the tangential strains very well.

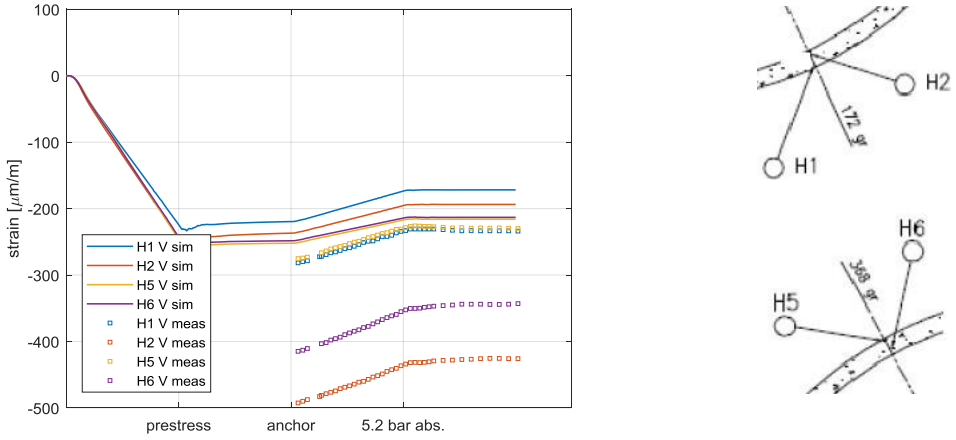

Figure 7: Comparison of simulated and measured vertical strain at sensors H1, H2, H5 and H6.

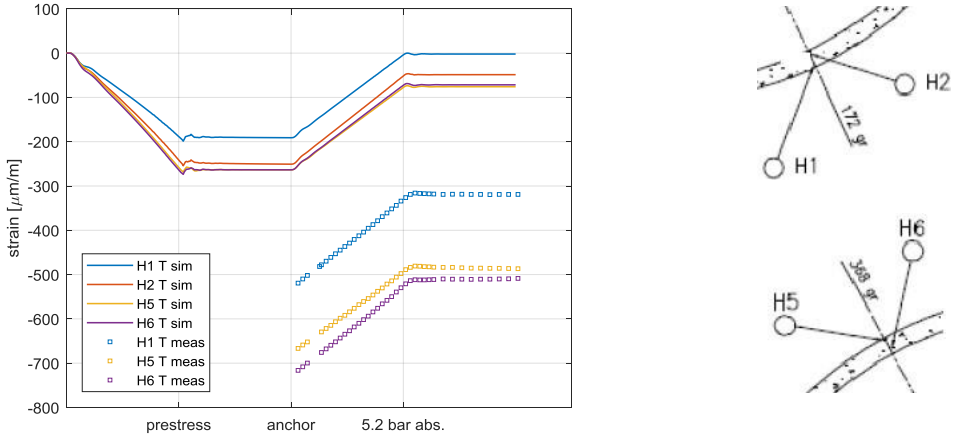

Figure 8: Comparison of simulated and measured tangential strain at sensors H1, H2, H5 and H6.

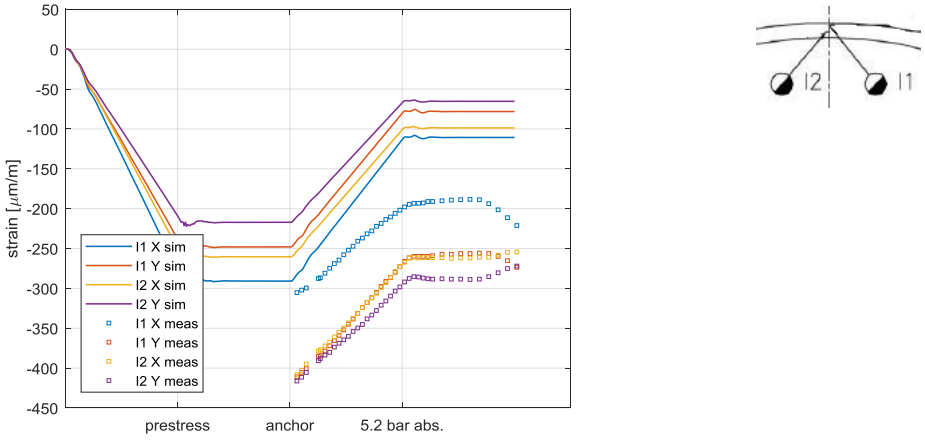

Figure 9: Comparison of simulated and measured strain in x- and y-direction at sensors I1 and I2.

Figure 10 summarizes the change of strain during the pressure increase comparing the simulated and the measured response for all available sensor signals. The sensors F1 Intrados Vertical and H2 Intrados Tangential broke during the construction and no evaluable signal could be retrieved. A good agreement of simulation and measurement is found. The biggest differences occur at the sensor F2 in the gusset region, because the special heat treatment was not yet simulated.

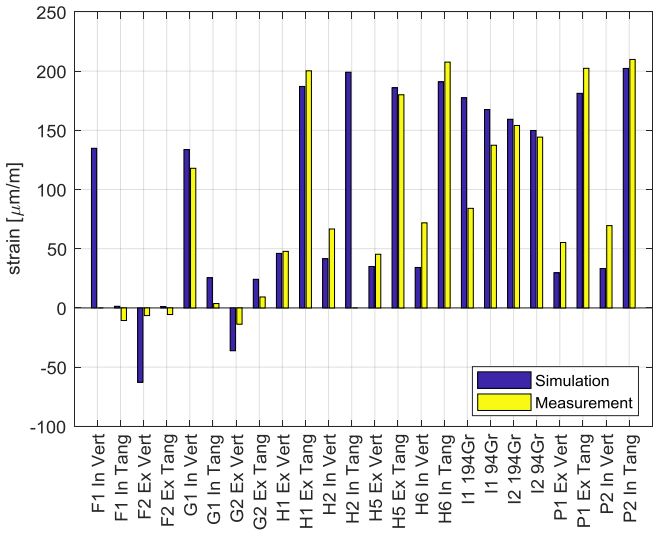

Figure 10: Simulated and measured change in concrete strain during the pressurization test for the sensors.

In addition to displacement and strain measurements a global and localized leakage measurement was performed during the first pressurization test of the VeRCoRs containment model. A total leak rate of 7.7 m³/h at standard conditions was recorded, whereby 56% of the leaked volume can be attributed to defects in the gusset region, 15% to defects in the hatch area, 25% to defect in the rest of the cylindrical wall and only 4% to defects in the dome. The high leakage value at the gusset results from a controlled heat treatment after the pouring of the concrete with the aim to generate cracks. EDF decided on the treatment explicitly and only for the gusset region. An inspection of the containment surface by EDF experts revealed, that leakage through clearly identifiable wall penetrating cracks occurred in the gusset region, whereby in the other regions leakage through enhanced porosity due to concrete damage was identified to be responsible.

On the basis of the structure mechanical simulation results a prediction method for the leakage through the damaged concrete structure was developed. LS-DYNA outputs besides nodal displacements and element stress and strain values additional concrete specific output quantities for the utilized MAT_172 concrete material model, in particular the current crack opening strain (COS). Figure 11 (a) displays COS at the end of the pressurization test for the whole concrete structure. In the simulation model 134 elements situated above and below the equipment hatch and in two regions within the dome exhibited a COS value significantly greater zero. The respective cracked elements near the equipment hatch are displayed in Figure 11 (b). Here, the simulation model possesses three stacked layers of thick shell elements due to the thickened wall design around the equipment hatch. Only the elements, where cracking is observed throughout the wall thickness, are considered. From these triples of elements the minimum COS value is then input in the cumulative leak rate calculation.

With the respective dimensions of the damaged concrete elements a crack width and length can be predicted on the basis of the COS value. The LS-DYNA Keyword User's Manual (2016) suggests the crack opening displacement (COD) to be computed by $COD = COS \cdot \sqrt{A}$, where A is the area of the

respective cracked shell element. Considering the crack length, the square root of the cracked element area can be used as an estimate. With a nominal element size of 0.2 m in our model and assuming one crack per element, COD of up to 0.45 mm appeared in the calculations, which are much bigger than the concrete cracks we expect to develop in the mock-up. A more accurate calculation of the crack dimensions would be possible, if the orientation angles of the cracks in respect to the element coordinate systems and the sensitivity of the crack dimensions on mesh refinement were investigated.

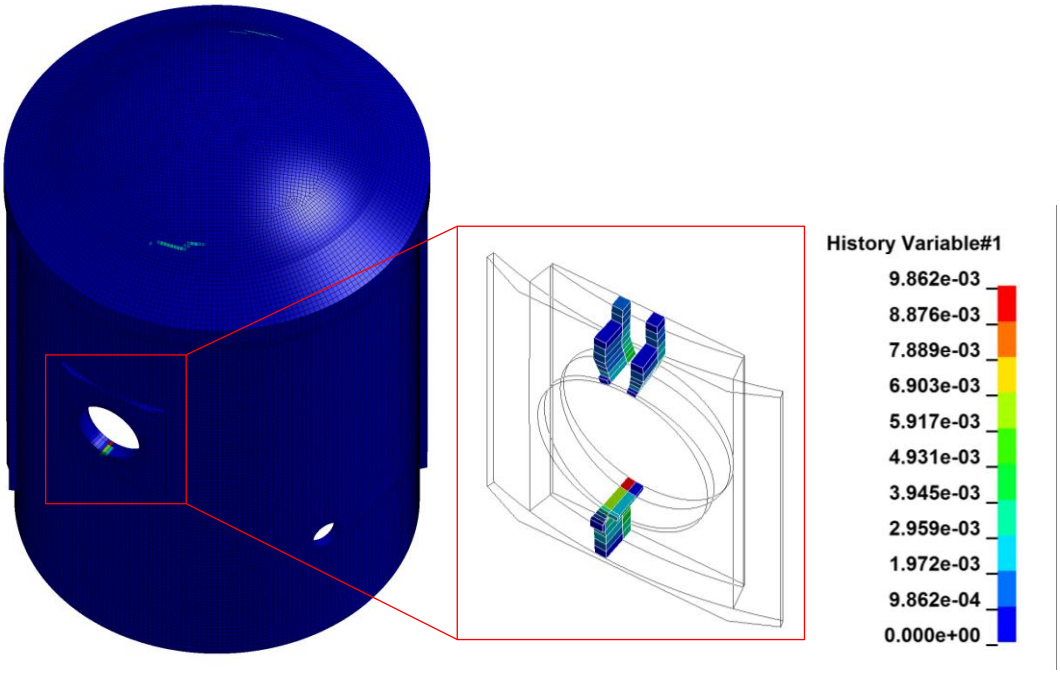

(a) (b)

Figure 11: Current crack opening strain at the end of the pressurization test in the whole containment (a) and the most severely damaged elements near the equipment hatch (b). The same scale is used in both plots.

Table 1 shows the measured and calculated leak rate values for the equipment hatch region. The calculated leak rate overestimates strongly the measured value, where the laminar flow estimation by Buss (1972) gives the most diverging result and the estimation by Gelain (2012) the best result.

Table 1: Comparison of measured and calculated local leak rates around the equipment hatch region during the pressurization test.

	Method	Leak rate [m³/h]
Measured	-	0.15*7.7 = 1.2
Calculated	Greiner and Ramm (1995)	26.9
	Rizkalla et al. (1984)	24.7
	Gelain (2012)	11.6
	Buss (1972)	60.2

The methods following Rizkalla et al. (1984) and Gelain (2012) take the Reynolds number of the leakage flow as input variable. Since the Reynolds number is not measured in the experiments only an estimate can be used in the calculations. During the pressurization test leakage through the dome was very low, which may partly be attributed to the stay-in-place formwork on the inside of the dome, which was assembled by precast concrete segments. In our view they may obstruct the leakage flow through the wall. Because the heat treatment of the gusset has not yet been included in the simulation, the concrete damage and cracking in the gusset region could not be reproduced. Considering the equipment hatch area the predicted locations of the leak flow, i.e. above and below the hatch, coincide well with the measurement results. Furthermore, the dominant leak flow value below the equipment hatch was reproduced in the simulation.

CONCLUSION AND OUTLOOK

The VeRCoRs containment model project is a new opportunity and challenge to study the integrity and leak-tightness of a pre-stressed concrete containment vessel also with regard to ageing aspects. We present structure mechanical simulations of the containment for a pressurization test. Simulation results compare well with the retrieved measurement data. Further research needs to be done on the prediction of the leak rate derived from concrete damage. Generally, a crack opening displacement calculation based on a concrete constitutive model with a smeared crack approach can only give a rough measure of the true crack pattern and crack dimensions. Element size plays a crucial role and we plan to conduct further studies on the element size sensitivity in respect to leak rate.

REFERENCES

Bahr, L., Sievers, J. (2013). "Structure mechanical simulation of a pre-stressed concrete containment vessel", *SMiRT-22 Transactions*, San Francisco, California, USA, paper 1078.

Buss, W. (1972) "Proof of leakage rate of a concrete reactor building", *Special Publication*, 34, 1291-1320.

Gelain, T. (2012) "An original method to assess leakage through cracked reinforced concrete walls", *Engineering Structures*, 38, 11-20.

Grebner, H., Sievers, J. (2005). "Structure Simulation of Pre-Stressed Concrete Containment Structures", *SMiRT 18 Transactions*, Beijing, China, paper H01-4.

Greiner, U., Ramm, W. (1995). "Air leakage characteristics in cracked concrete", *Nuclear Engineering and Design*, 156, 167-172.

Hessheimer, M.F., Klamerus, E.W., Lambert, L.D., Rightley, G.S. (2003). "Over-pressurization Test of a 1:4-Scale Prestressed Concrete Containment Vessel Model", *NUREG/CR-6810*, U.S. Nuclear regulatory commission (NRC).

Hessheimer, M.F., Dameron, R.A. (2006). „Containment Integrity Research at Sandia National Laboratories - An Overview," *NUREG/CR-6906*, U.S. Nuclear regulatory commission (NRC).

LS-DYNA R9.0.1 (2016) Livermore Software Technology Corporation (LSTC), http://www.lstc.com/.

LS-DYNA Keyword User's Manual – Volume II: Material Models (2016). Livermore Software Technology Corporation (LSTC), http://www.lstc.com/download/manuals.

NEA/CSNI/R(2004)11. "International Standard Problem No.48 - Containment Capacity. Phase 2 Report - Results of Pressure Loading Analysis," *OECD Nuclear Energy Agency (NEA)*, http://www.oecd-nea.org/nsd/docs/indexcsni.html.

Rizkalla, S. H., Lau, B. L., Simmonds, S. H. (1984) "Air leakage characteristics in reinforced concrete", *Journal of Structural Engineering*, 110, 1149-1162.

Standard Problem Exercise #3 – Round-Robin Analysis on Containment Performance (SPE #3) (2010), *Sandia National Laboratories*, http://www.sandia.gov/spe3/index.html.